Finite-Temperature Effects on Gluon Screening Masses in Dense Two-Color QCD

Speaker : Kei Tohme[1]

Collab. in

Kei Iida[2,3], Etsuko Itou[4,5], Daiki Suenaga[6] , Hideo Suganuma[1] and Atsuya Tokutake[1]

[1] Kyoto University, [2] The Open University of Japan, [3] RIKEN Nishina Center, [4] YITP (Kyoto), [5] RIKEN iTHEMS, [6] Nagoya University KMI

July 31st, 2026@ Lattice 2026(Maryland, US)

Phase diagram of QC_2D

K. Iida, E. Itou, K. Murakami, D. Suenaga, JHEP 2024, 2024, 22.

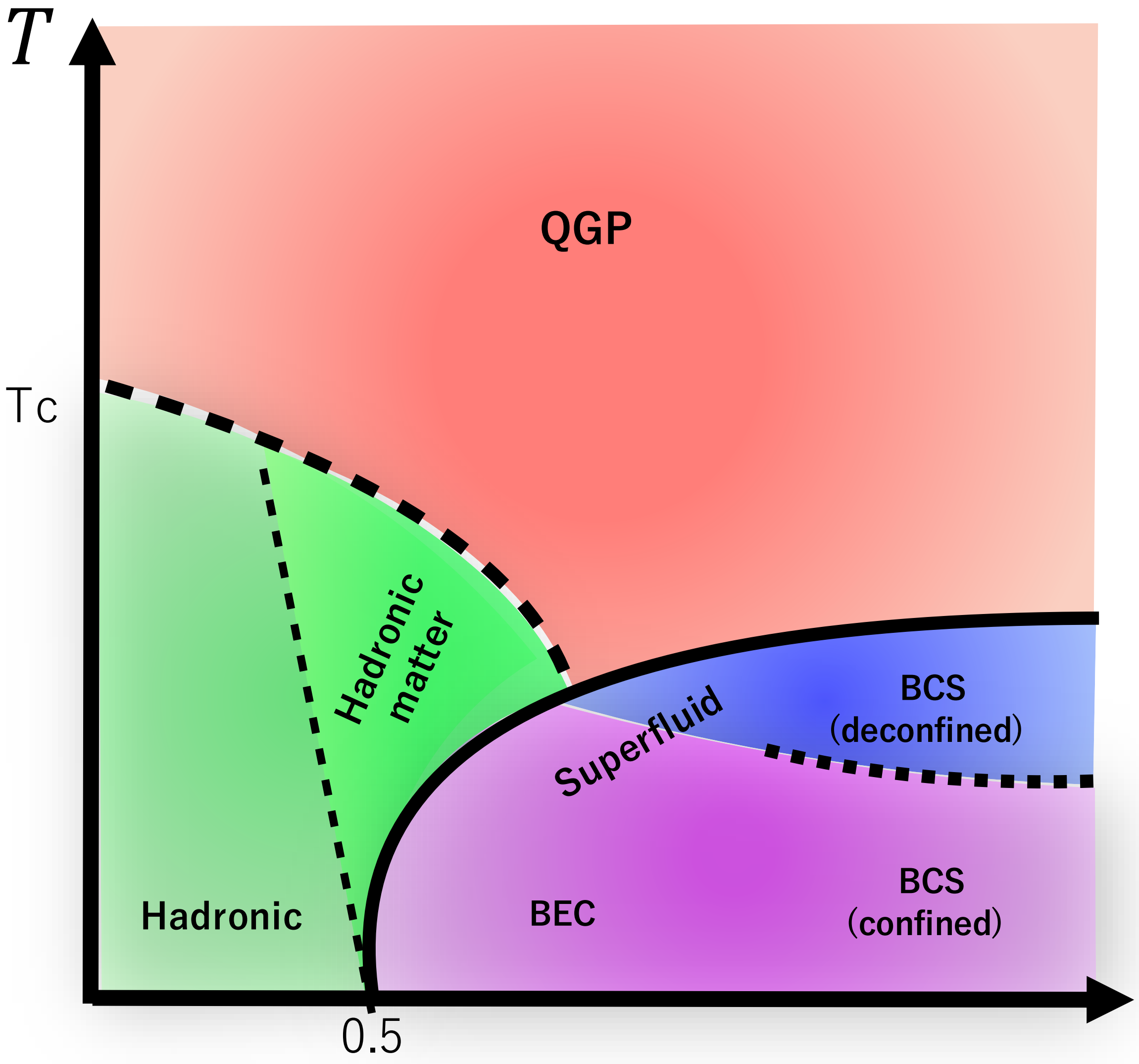

In 2-color QCD (QC_2D), lattice calculation can access to the finite-density region.

μ/M_π $\boldsymbol{M_\pi \simeq 738\,\mathrm{MeV}}$ $(aM_\pi = 0.620)$

Phase diagram of QC_2D

K. Iida, E. Itou, K. Murakami, D. Suenaga, JHEP 2024, 2024, 22.

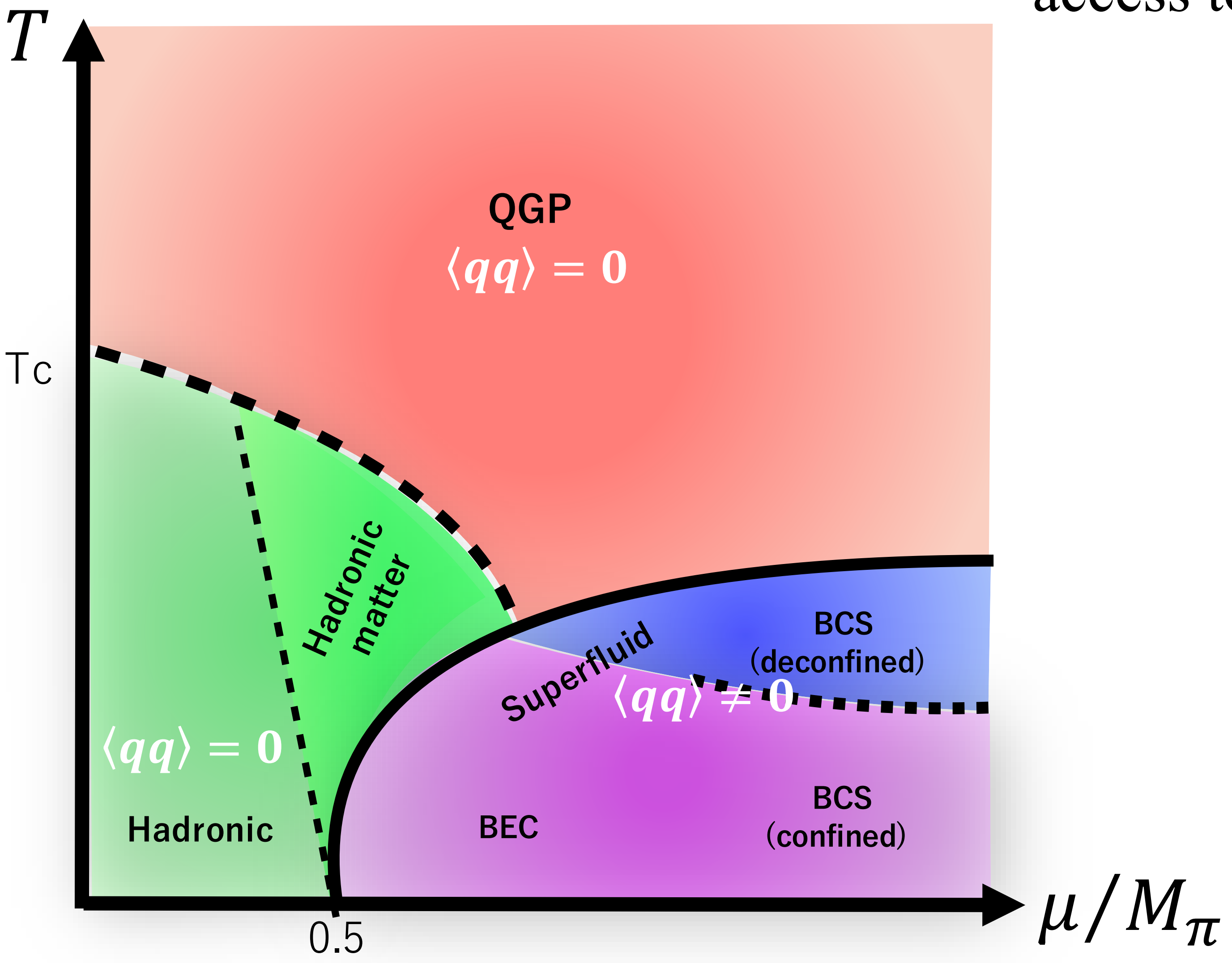

In 2-color QCD (QC_2D), lattice calculation can access to the finite-density region.

$\boldsymbol{M_\pi \simeq 738\,\mathrm{MeV}}$ $(aM_\pi = 0.620)$

Phase diagram of QC_2D

K. Iida, E. Itou, K. Murakami, D. Suenaga, JHEP 2024, 2024, 22.

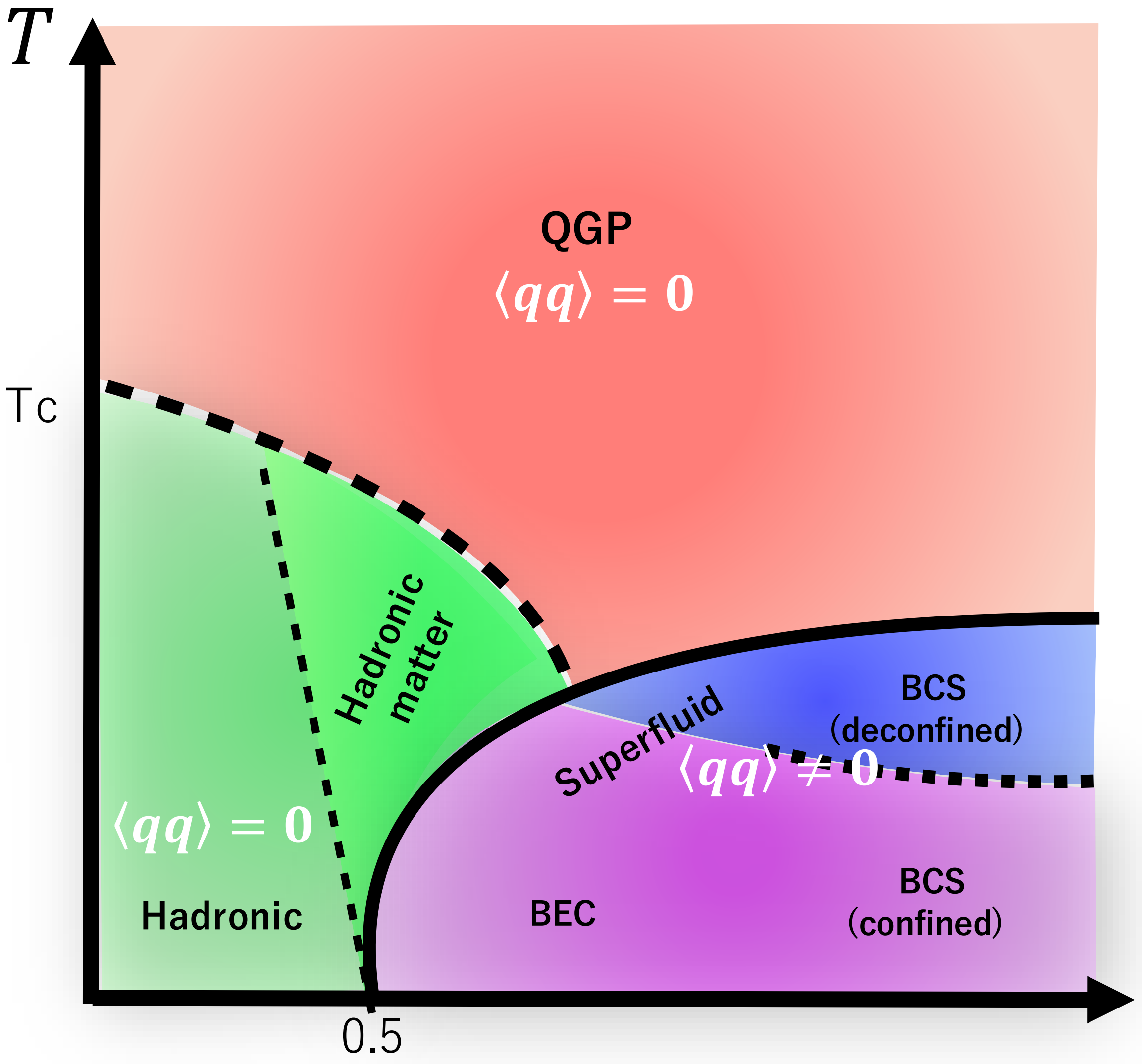

In 2-color QCD (QC_2D), lattice calculation can access to the finite-density region.

Studies so far:
Low temperatures ($T \approx$80MeV, 40MeV)

This study:
high temperature ($T >$100 MeV)

$\boldsymbol{M_\pi \simeq 738\,\mathrm{MeV}}$ $(aM_\pi = 0.620)$

Lattice Setup

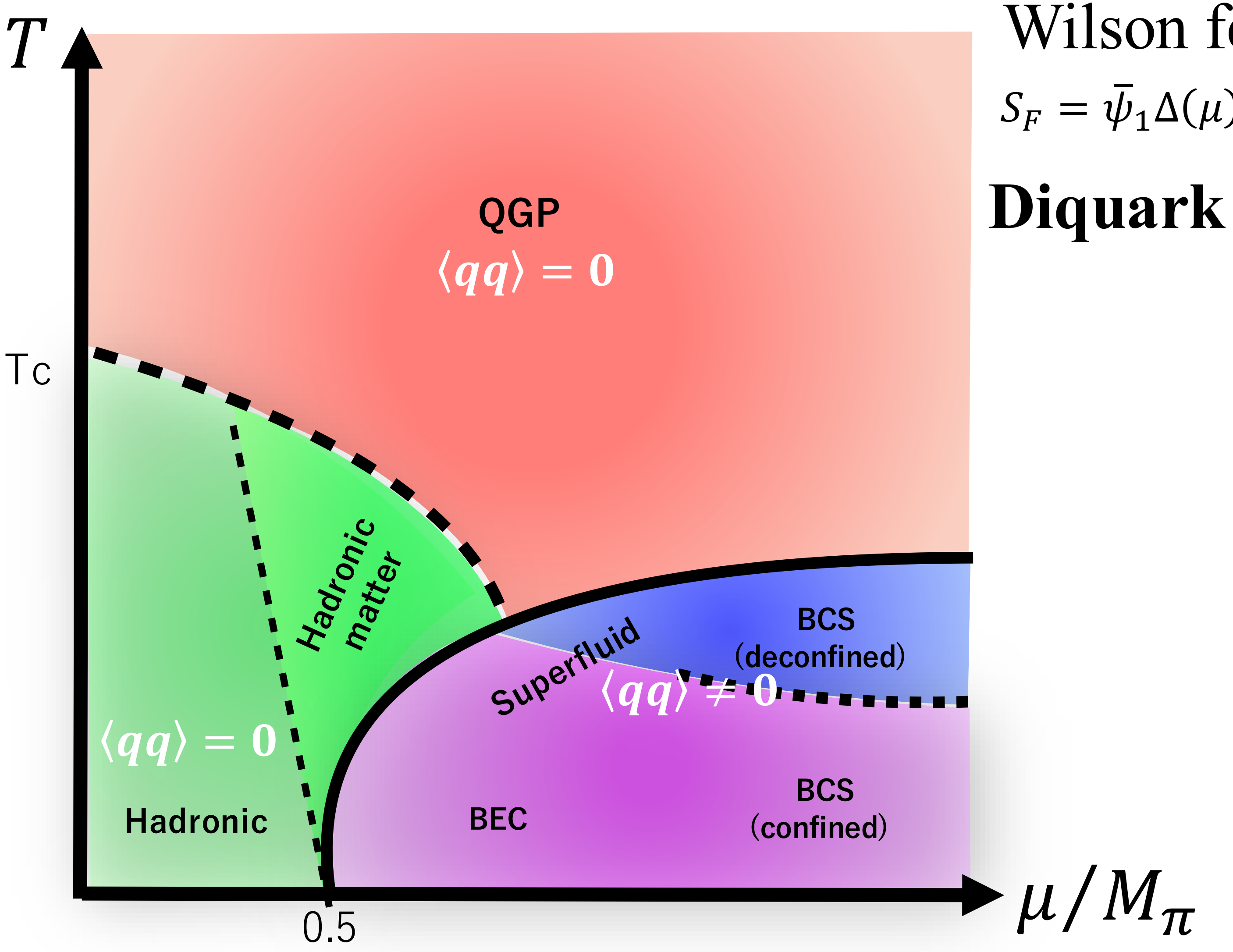

2 flavor QC₂D:

Iwasaki gauge action ($\beta = 0.80$),

Wilson fermion ($\kappa = 0.1590$).

$$S_F = \bar{\psi}_1 \Delta(\mu)\psi_1 + \bar{\psi}_2 \Delta(\mu)\psi_2 - J\,\bar{\psi}_1 (C\gamma_5)\tau_2 \bar{\psi}_2^T + J\psi_2^T (C\gamma_5)\tau_2 \psi_1$$

Diquark source ($J = j\kappa,\ aj =$0.010, 0.015, 0.020).

$\boldsymbol{M_\pi \simeq}$ **738 MeV** ($aM_\pi = 0.620$)

Lattice Setup

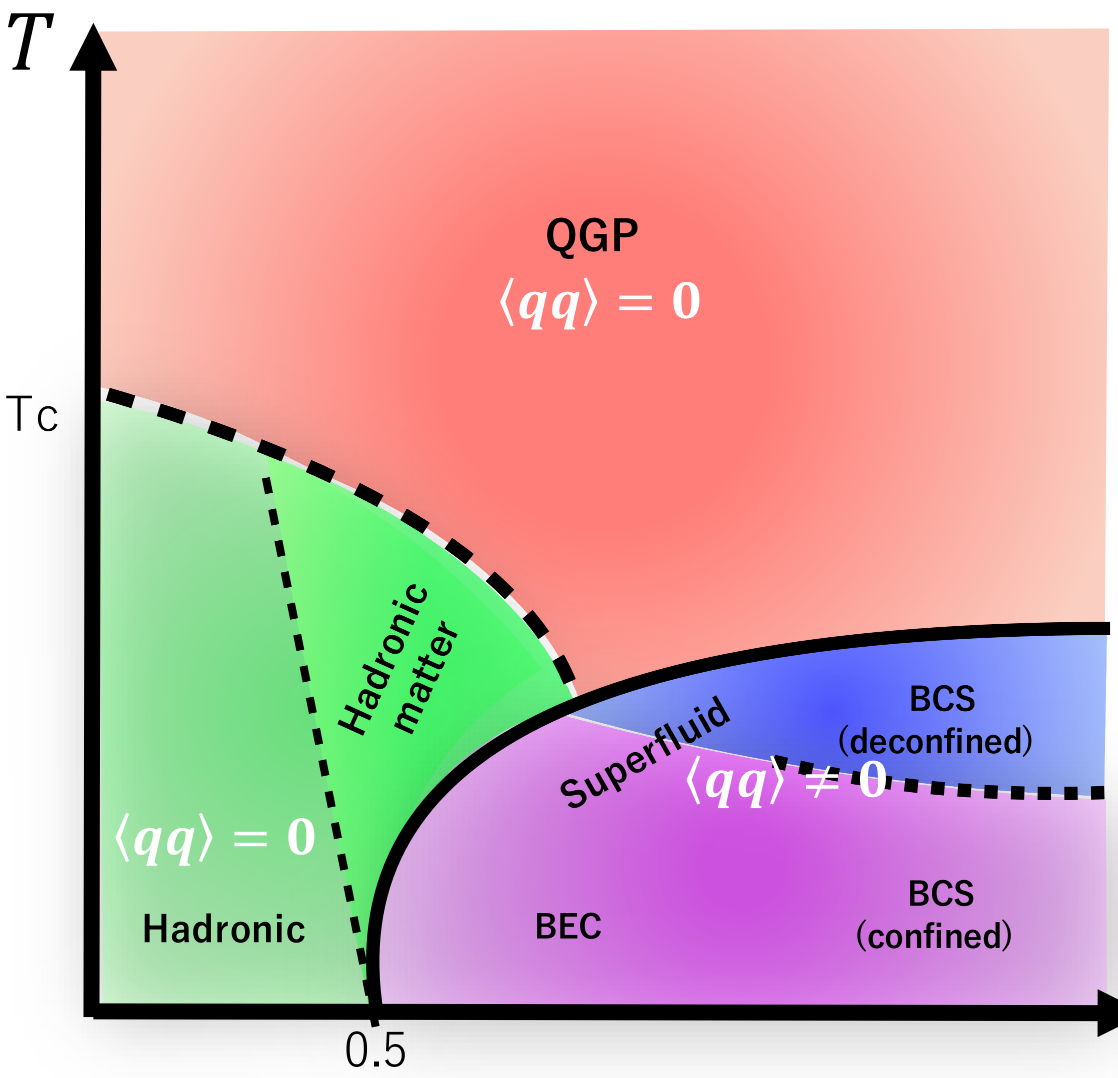

2 flavor QC_2D:

Iwasaki gauge action ($\beta = 0.80$),

Wilson fermion ($\kappa = 0.1590$).

$S_F = \bar{\psi}_1 \Delta(\mu) \psi_1 + \bar{\psi}_2 \Delta(\mu) \psi_2 - J\, \bar{\psi}_1 (C\gamma_5) \tau_2 \bar{\psi}_2^T + J \psi_2^T (C\gamma_5) \tau_2 \psi_1$

Diquark source ($J = j\kappa,\ aj =$0.010, 0.015, 0.020).

→Scan various $a\mu$ ($a\mu \in [0.00, 0.75]$).

Lattice size:

$32^3 \times 10$ (~124 MeV)

$32^3 \times 12$ (~103 MeV), $32^3 \times 32$ (~ 39 MeV)

μ / M_π $\quad$ $\boldsymbol{M_\pi \simeq 738}$ **MeV** ($aM_\pi = 0.620$)

Lattice Setup

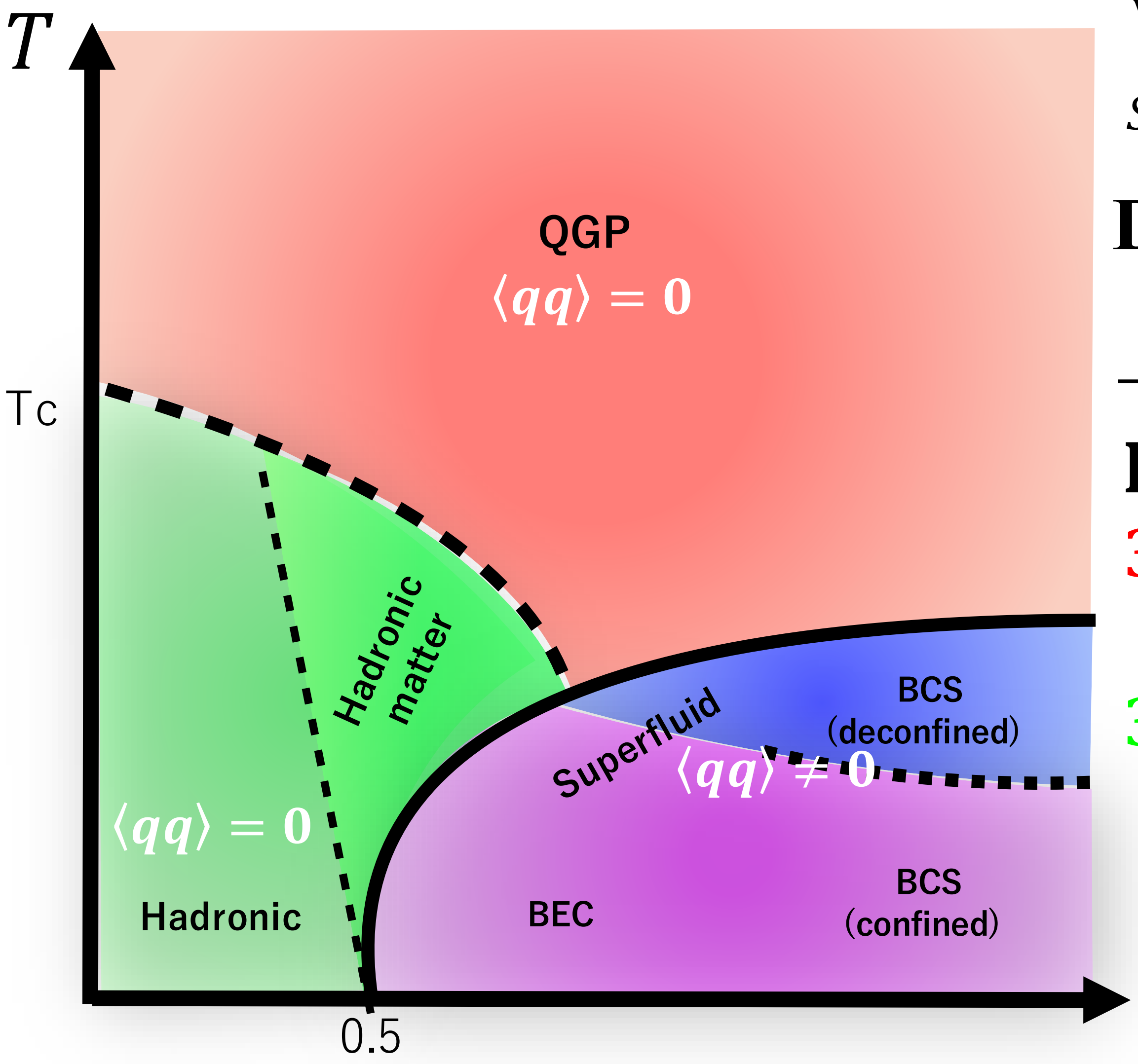

2 flavor QC_2D:
Iwasaki gauge action ($\beta = 0.80$),
Wilson fermion ($\kappa = 0.1590$).

$$S_F = \bar{\psi}_1\Delta(\mu)\psi_1 + \bar{\psi}_2\Delta(\mu)\psi_2 - J\,\bar{\psi}_1(C\gamma_5)\tau_2\bar{\psi}_2^T + J\psi_2^T(C\gamma_5)\tau_2\psi_1$$

Diquark source ($J = j\kappa,\ aj =$0.010, 0.015, 0.020).

→Scan various $a\mu$ ($a\mu \in [0.00, 0.75]$).

Lattice size:

$32^3 \times 10$ (~124 MeV)
  $j = 0$ calc. is doable in whole μ.

$32^3 \times 12$ (~103 MeV), $32^3 \times 32$ (~ 39 MeV)
  $j \neq 0$ calc. is needed in $\mu/M_\pi \gtrsim 0.5$.

μ/M_π **$M_\pi \simeq$ 738 MeV** ($aM_\pi = 0.620$)

Lattice Setup

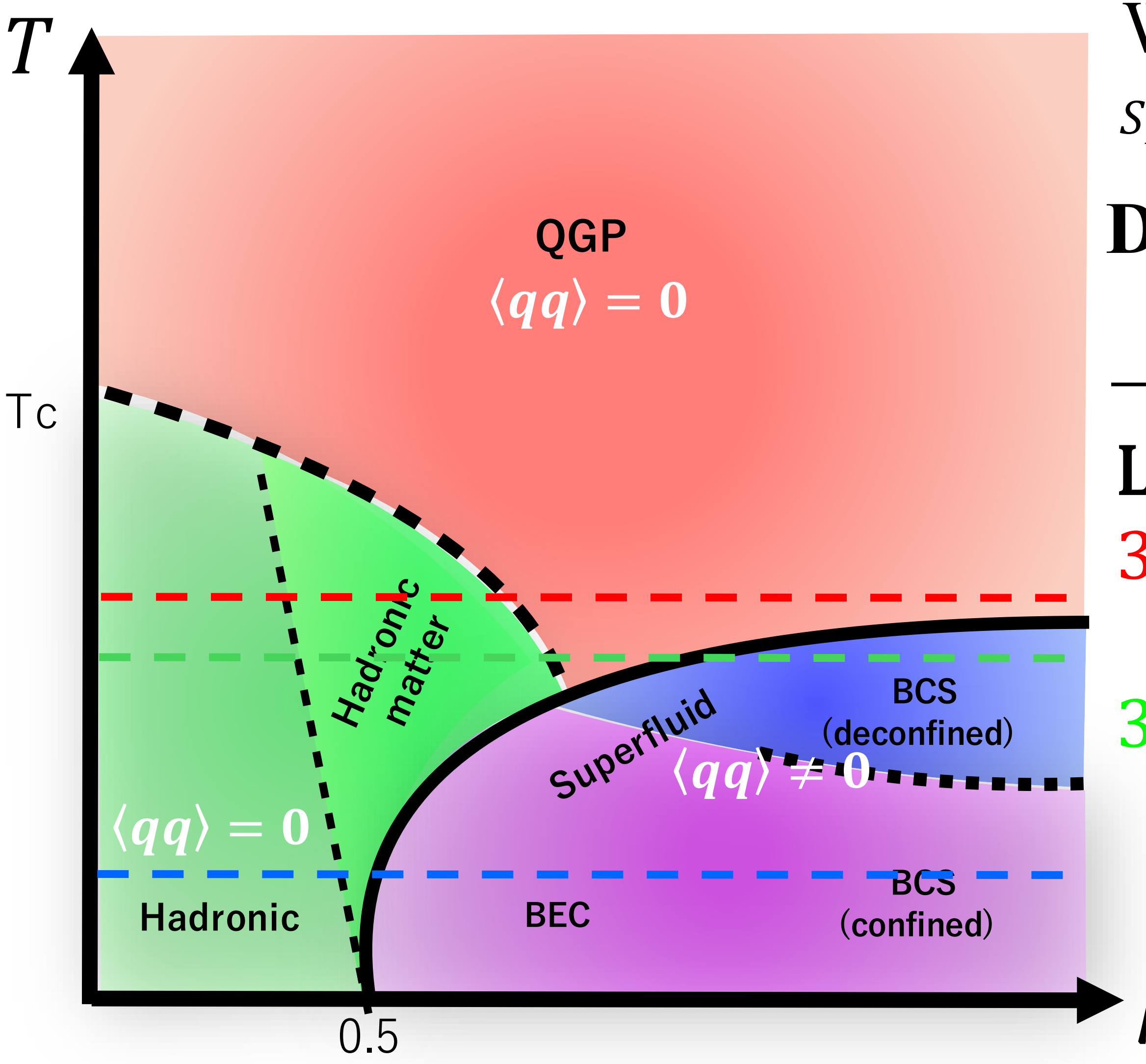

2 flavor QC$_2$D:
Iwasaki gauge action ($\beta = 0.80$),
Wilson fermion ($\kappa = 0.1590$).

$$S_F = \bar{\psi}_1 \Delta(\mu) \psi_1 + \bar{\psi}_2 \Delta(\mu) \psi_2 - J\, \bar{\psi}_1 (C\gamma_5) \tau_2 \bar{\psi}_2^T + J \psi_2^T (C\gamma_5) \tau_2 \psi_1$$

Diquark source ($J = j\kappa,\ aj =$0.010, 0.015, 0.020).

→Scan various $a\mu$ ($a\mu \in [0.00, 0.75]$).

Lattice size:

$32^3 \times 10$ (~124 MeV)
$j = 0$ calc. is doable in whole μ.
$32^3 \times 12$ (~103 MeV), $32^3 \times 32$ (~ 39 MeV)
$j \neq 0$ calc. is needed in $\mu/M_\pi \gtrsim 0.5$.

$\boldsymbol{M_\pi \simeq 738}$ **MeV** ($aM_\pi = 0.620$)

Polyakov loop on a T-μ plane

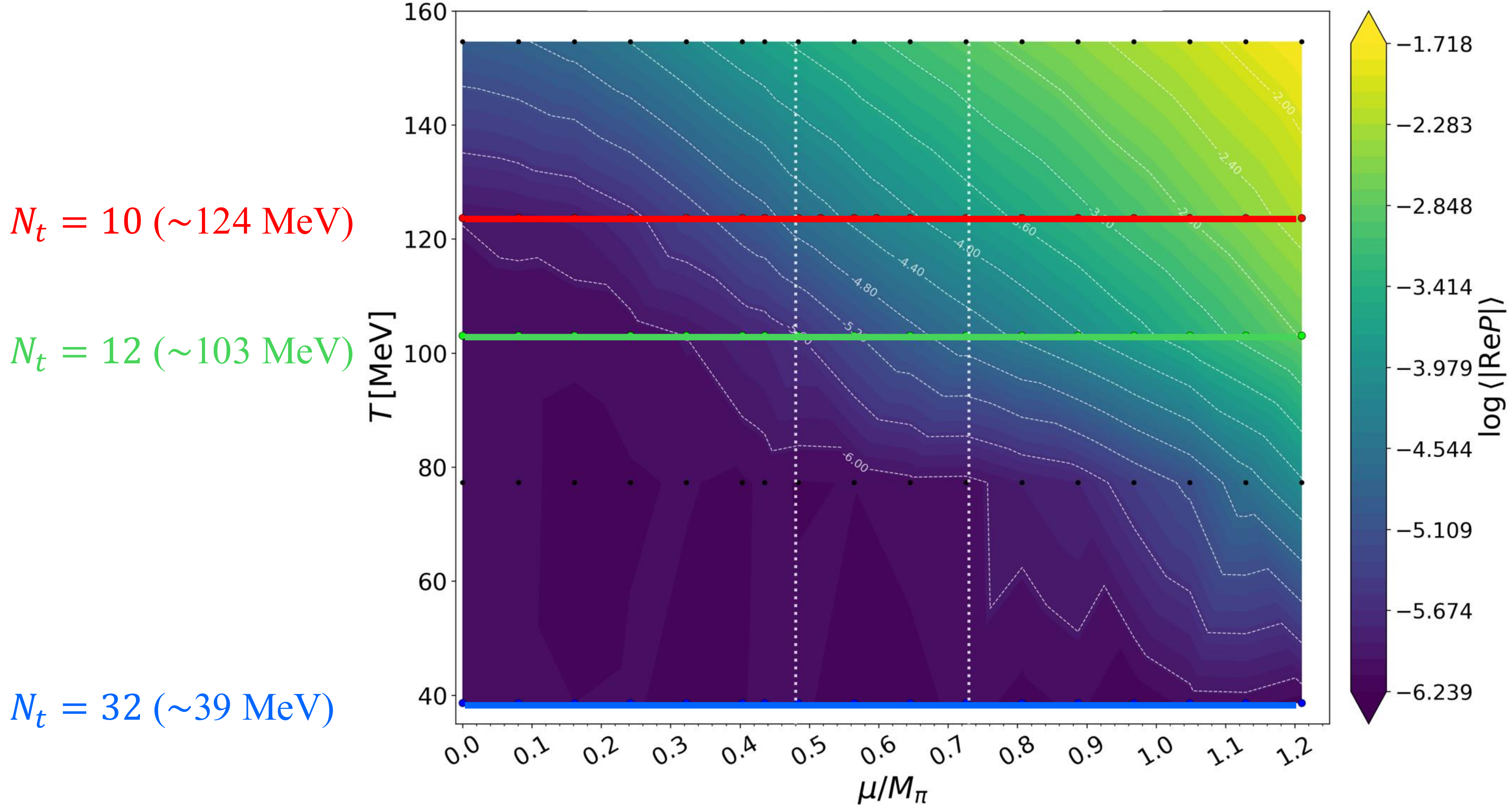

At $N_t = 32$, confinement remains in whole μ region.

At $N_t = 10,12$, deconfinement occurs in high μ region.

More precise phase diagram in this study

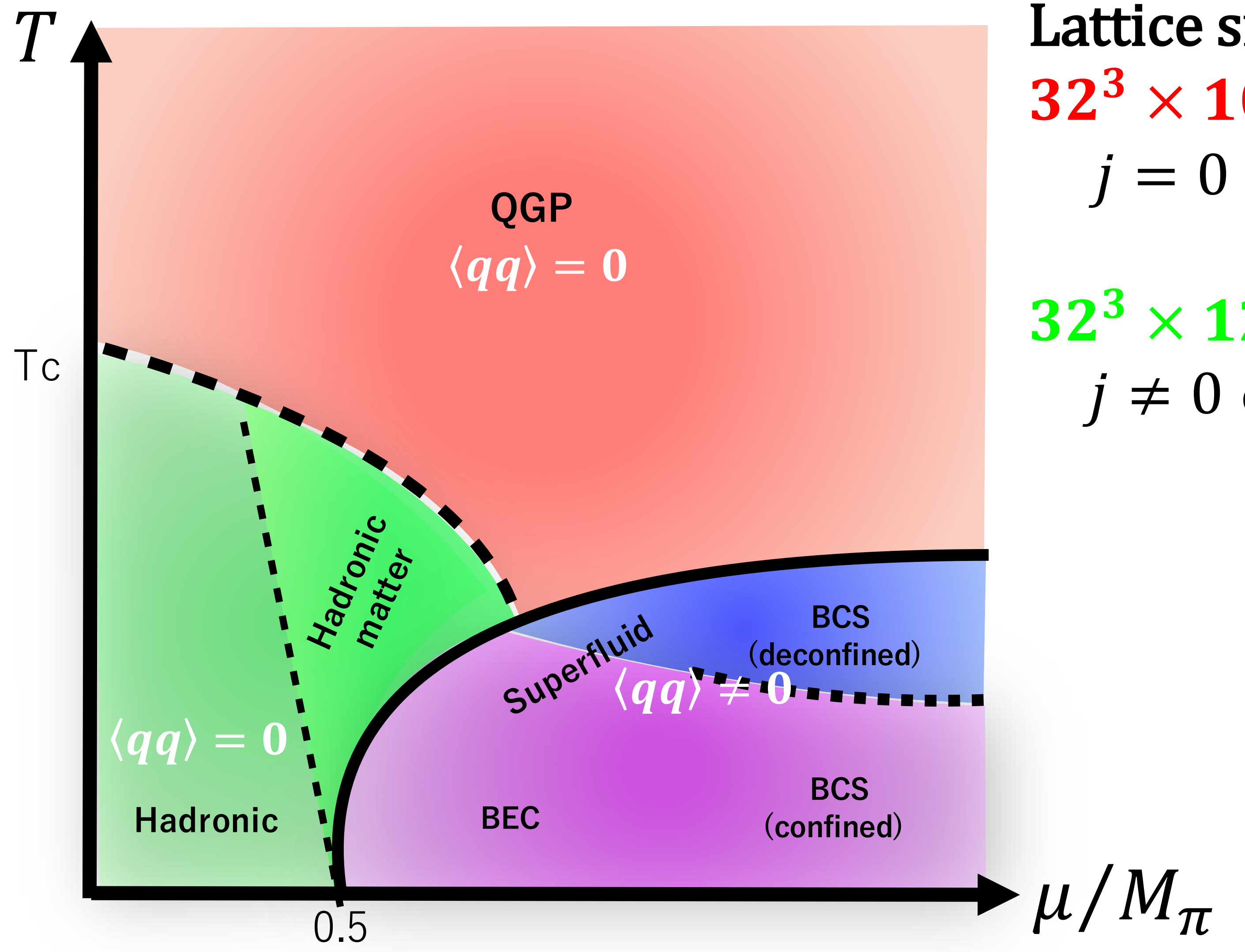

Lattice size:

$\mathbf{32^3 \times 10}$ **(~124 MeV)**

$j = 0$ calc. is doable in whole μ.

$\mathbf{32^3 \times 12}$ **(~103 MeV)**, $\mathbf{32^3 \times 32}$ **(~ 39 MeV)**

$j \neq 0$ calc. is needed in $\mu/M_\pi \gtrsim 0.5$.

$\boldsymbol{M_\pi \simeq 738}$ **MeV** $(aM_\pi = 0.620)$

More precise phase diagram in this study

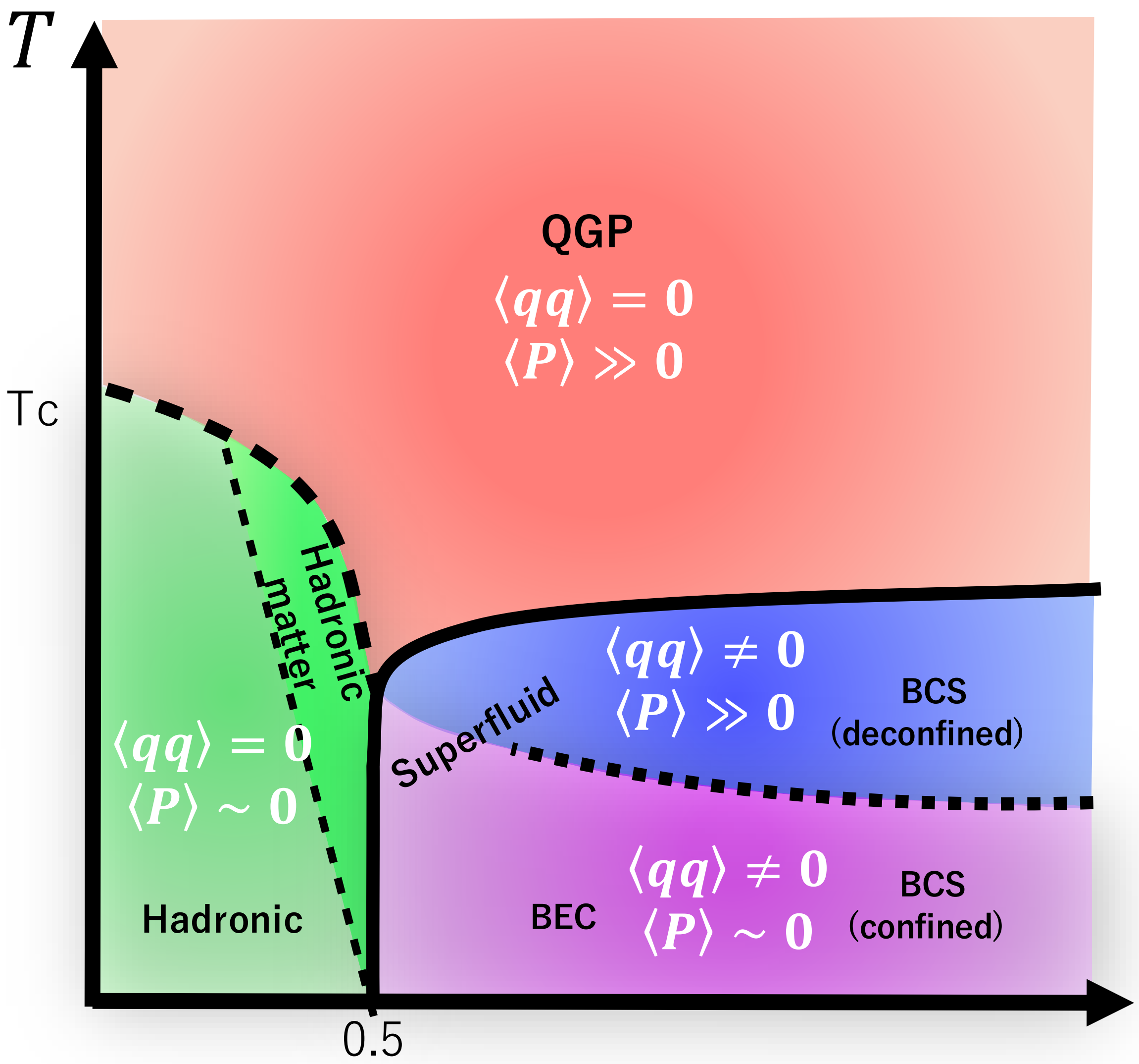

Lattice size:

$32^3 \times 10$ (~124 MeV)

$j = 0$ calc. is doable in whole μ.

$32^3 \times 12$ (~103 MeV), **$32^3 \times 32$ (~ 39 MeV)**

$j \neq 0$ calc. is needed in $\mu/M_\pi \gtrsim 0.5$.

$\boldsymbol{M_\pi \simeq 738}$ **MeV** $(aM_\pi = 0.620)$

More precise phase diagram in this study

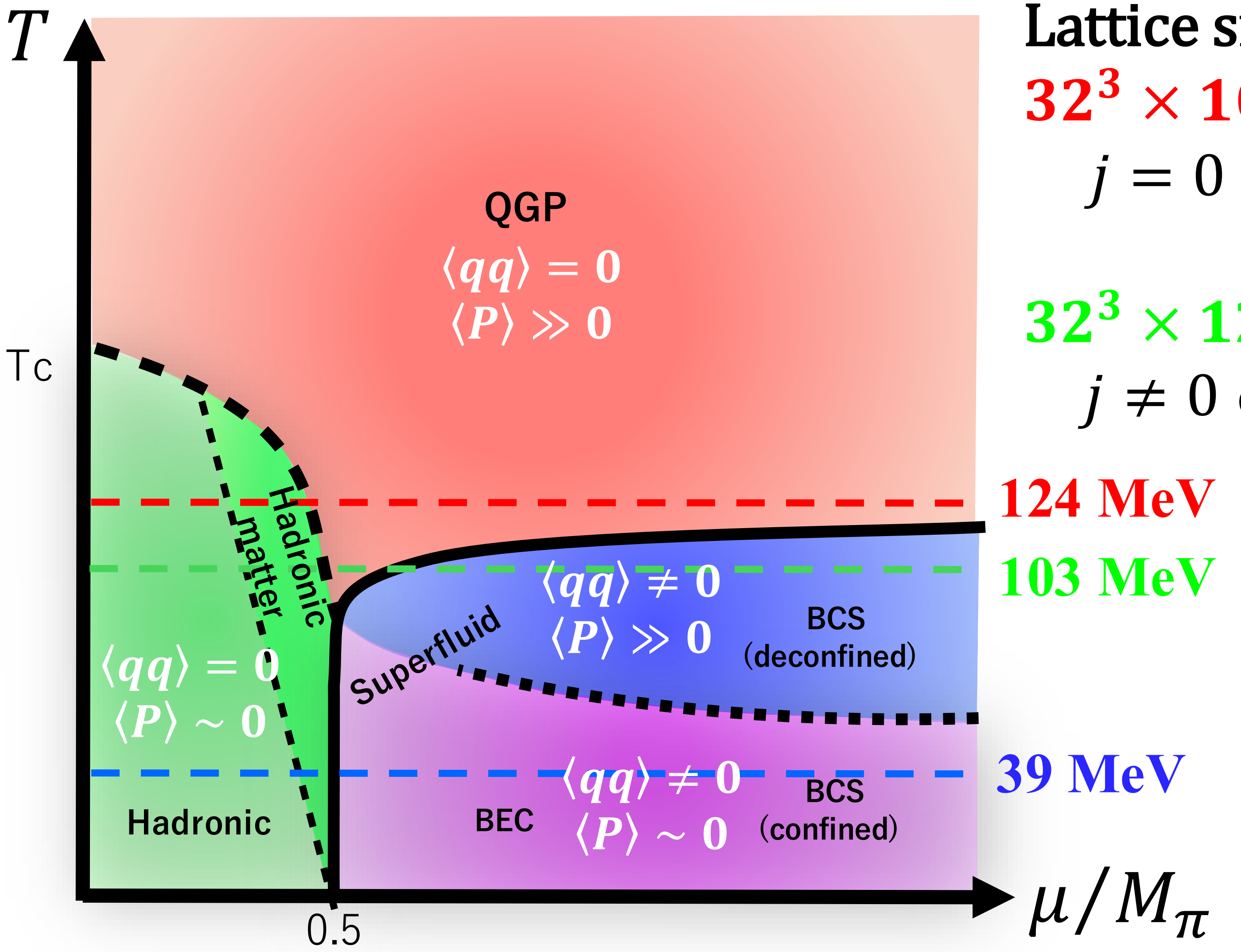

Lattice size:

$32^3 \times 10$ (~124 MeV)

$j = 0$ calc. is doable in whole μ.

$32^3 \times 12$ (~103 MeV), $32^3 \times 32$ (~ 39 MeV)

$j \neq 0$ calc. is needed in $\mu/M_\pi \gtrsim 0.5$.

$\boldsymbol{M_\pi \simeq 738}$ **MeV** $(aM_\pi = 0.620)$

More precise phase diagram in this study

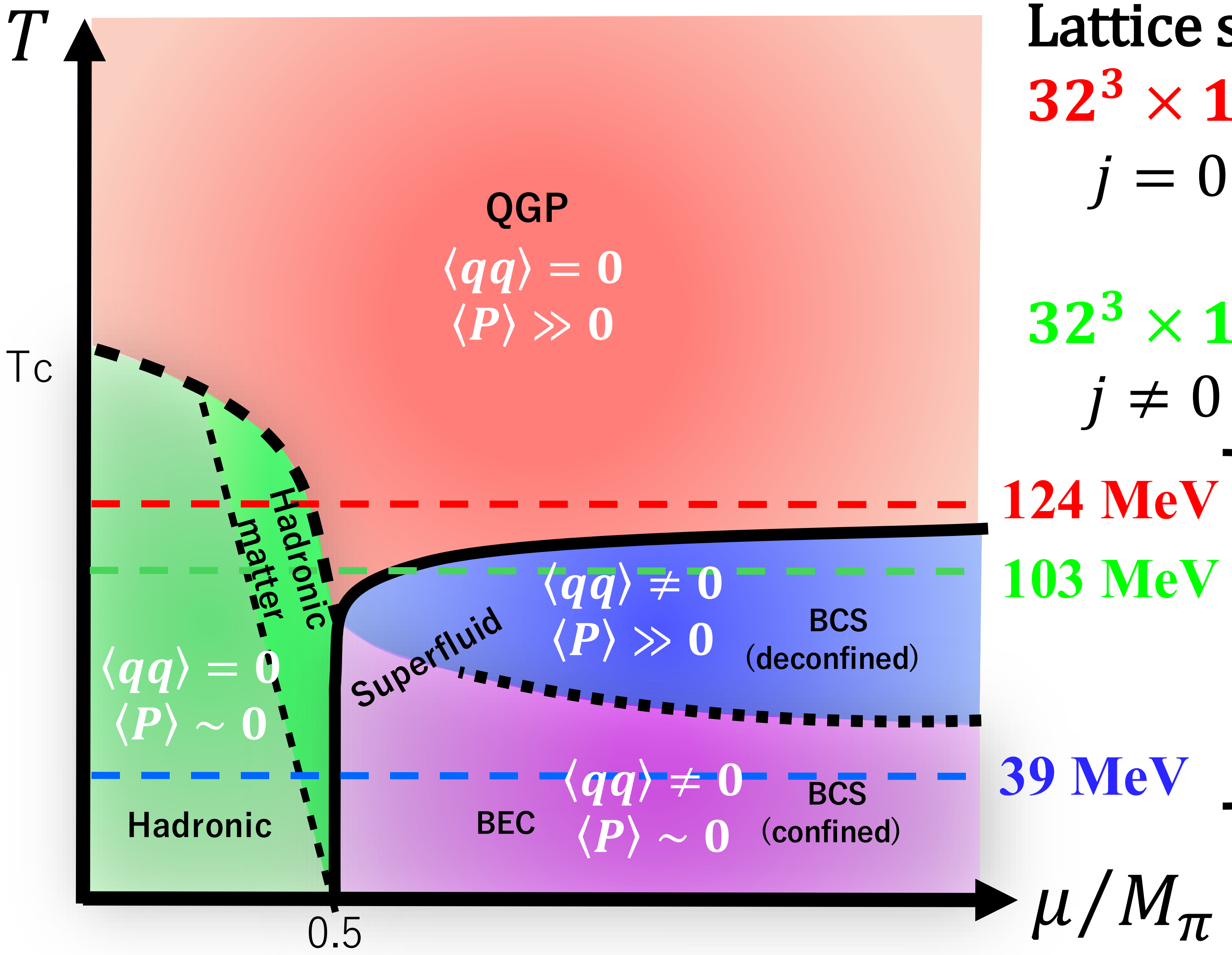

Lattice size:

$32^3 \times 10$ (~124 MeV)

$j = 0$ calc. is doable in whole μ.

$32^3 \times 12$ (~103 MeV), $32^3 \times 32$ (~ 39 MeV)

$j \neq 0$ calc. is needed in $\mu / M_\pi \gtrsim 0.5$.

Investigate gluon sector!

$\boldsymbol{M_\pi \simeq 738}$ **MeV** $(aM_\pi = 0.620)$

What other gluonic observables exhibit μ dependence?

Gluonic observables:

- **Polyakov loop** (already checked)
- **Gluon propagator and screening mass**

Indeed, the previous studies on gluon mass show inconsistent results.

UK group: T. Boz, et al., Phys. Rev. D **99**, 074514(2019)

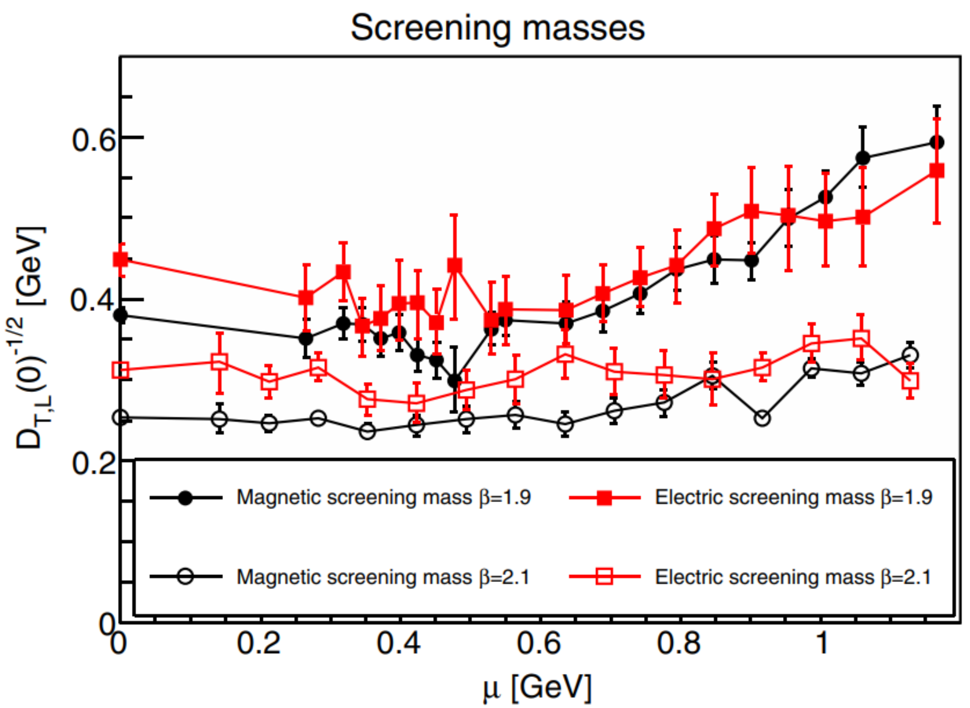

Russian group : V. G. Bornyakov, et al., Phys. Rev. D **102**, 114511 (2020)

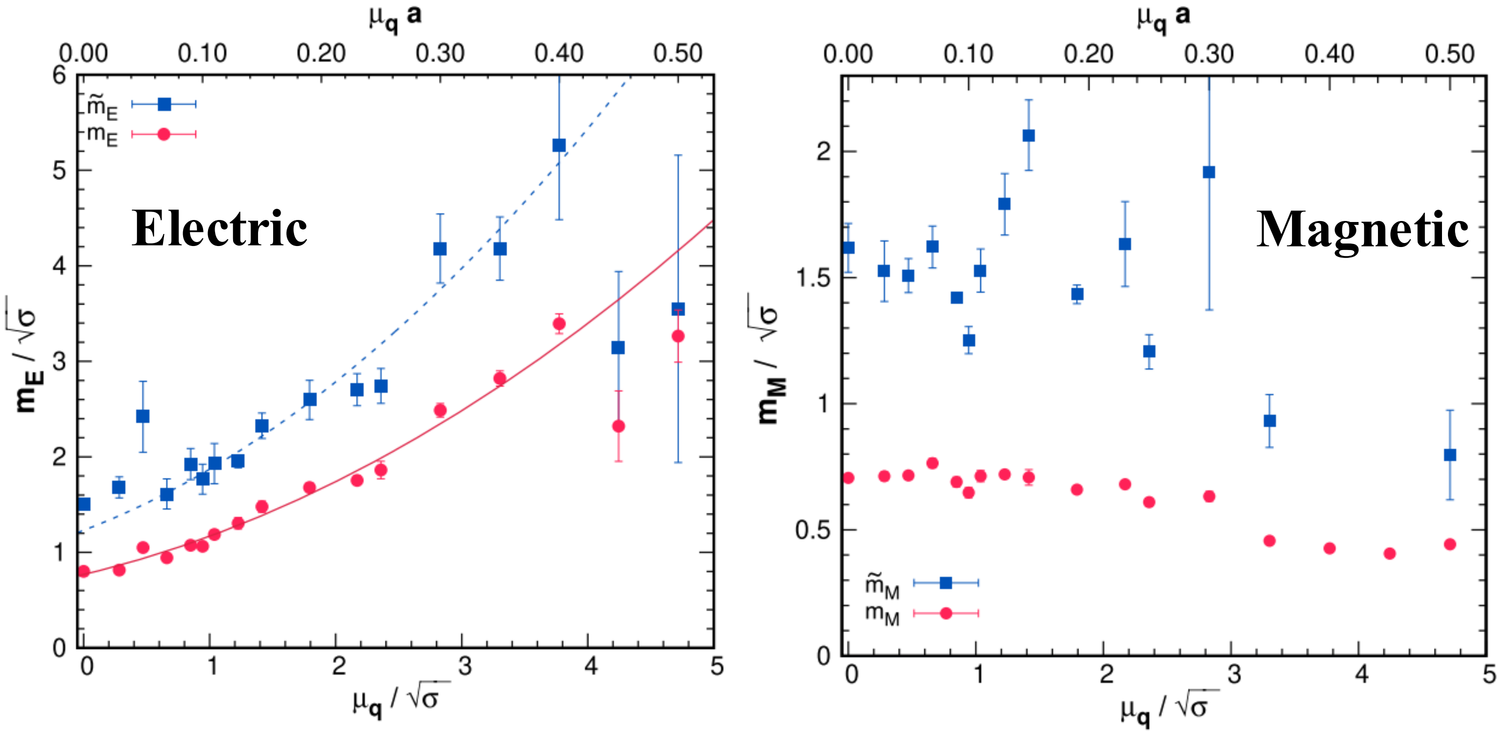

Different μ-dependences… Why?

Gluon propagator and screening mass

Gluon propagator (Landau gauge in finite *T*):

$$\left(\tilde{A}_\mu(p) \equiv \int dx^d A_\mu(x) e^{ipx} \right)$$

$$D_{\mu\nu}(p) \equiv \langle \tilde{A}_\mu(p) \tilde{A}_\nu(-p) \rangle$$
$$= P^{\mathrm{T}}_{\mu\nu} D_{\mathrm{T}}(p_0, \vec{p}) + P^{\mathrm{L}}_{\mu\nu} D_L(p_0, \vec{p}),$$

$$P^{\mathrm{T}}_{\mu\nu} = (1 - \delta_{\mu 0})(1 - \delta_{\nu 0}) \left(\delta_{\mu\nu} - \frac{p_\mu p_\nu}{\vec{p}^2} \right), \qquad P^{\mathrm{L}}_{\mu\nu} = \left(\delta_{\mu\nu} - \frac{p_\mu p_\nu}{p^2} \right) - P^{\mathrm{T}}_{\mu\nu}.$$

Dressing function:

Magnetic: $D_{\mathrm{T}}(p_0, \vec{p}) = \frac{1}{(d-2)N_g} \left\langle \sum_{i=1}^{3} \tilde{A}_i(p) \tilde{A}_i(-p) - \frac{p_0^2}{\vec{p}^2} \tilde{A}_0(p) \tilde{A}_0(-p) \right\rangle,$

Electric: $D_L(p_0, \vec{p}) = \frac{1}{N_g} \left(1 + \frac{p_0^2}{\vec{p}^2} \right) \langle \tilde{A}_0(p) \tilde{A}_0(-p) \rangle.$

Gluon screening mass:

$$\boldsymbol{M}_{\mathbf{T/L}} \equiv \frac{\mathbf{1}}{\sqrt{\boldsymbol{D}_{\mathbf{T/L}}(0, \vec{\mathbf{0}})}}$$

Calculation strategy of gluon propagator

1. Generate the gauge configurations $\{U_\mu(x)\}$ in SU(2) color lattice simulation.
2. Perform the Landau gauge fixing so as to maximize

$$\sum_x \mathrm{ReTr}\left[\sum_{\mu=1}^{4} U_\mu(x)\right].$$

3. Extract gauge fields $A_\mu(x)$ from $U_\mu(x)$ and perform Fourier transf. to get $\tilde{A}_\mu(p)$.
4. Calculate 2pt functions $\langle \tilde{A}_\mu(p)\tilde{A}_\mu(-p)\rangle$ and extract means and errors (jackknife).

   We calculate the transverse and longitudinal propagators as

$$\boldsymbol{D_T(0,\vec{0}) = \frac{1}{2N_g}\sum_{k=1}^{3}\langle \tilde{A}_k(0)\tilde{A}_k(0)\rangle}, \quad \boldsymbol{D_L(0,\vec{0}) = \frac{1}{N_g}\langle \tilde{A}_0(0)\tilde{A}_0(0)\rangle}.$$

5. At high density, perform extrapolation for j to 0.

Chemical potential dependence of gluon propagator

Magnetic propagator $D_T(0,\vec{p})$: ***Dark*** *Small μ* $\boldsymbol{\mu}$ ***Bright*** *Large μ*

After taking the linear extrapolation in *j* **:**

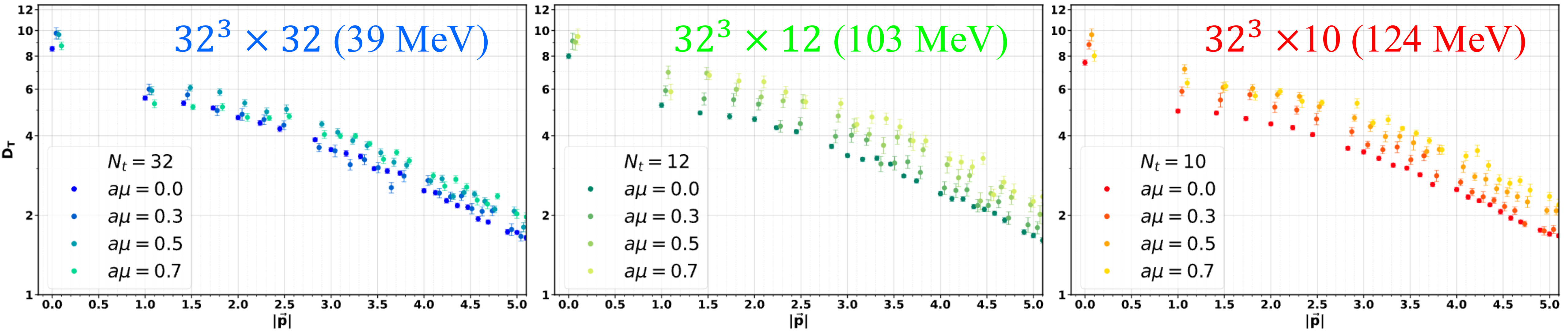

At low temperature (T = 39 MeV): $\boldsymbol{D_T(0,\vec{p})}$ **does not depend on $\boldsymbol{\mu}$ so much.**

At high temperature (T = 103,124 MeV): $\boldsymbol{D_T(0,\vec{p})}$ ***increase*** **as $\boldsymbol{\mu}$ increases.**

Chemical potential dependence of gluon propagator

Electric propagator $D_L(0,\vec{p})$: ***Dark*** *Small μ* $\boldsymbol{\mu}$ ***Bright*** *Large μ*

After taking the linear extrapolation in j :

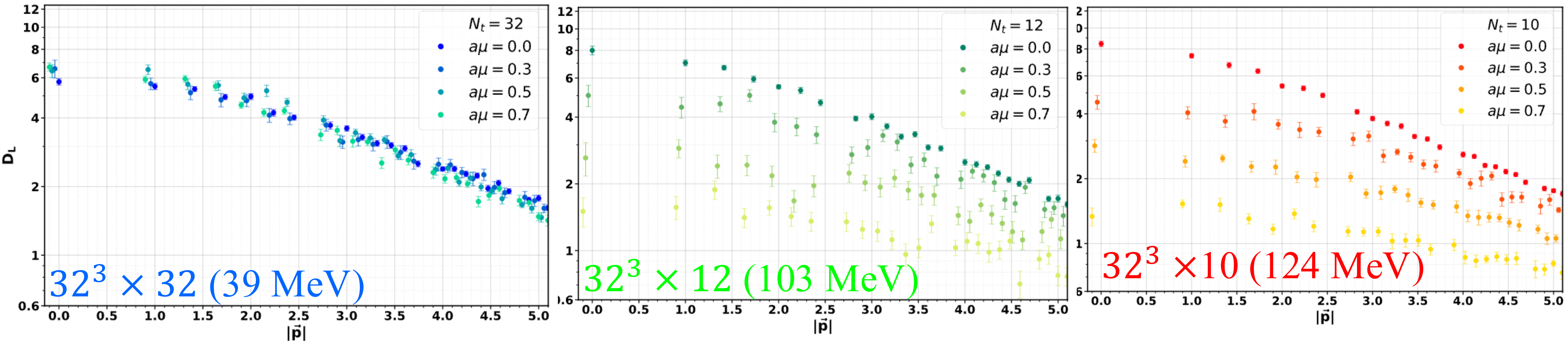

At low temperature ($T = 39$ MeV): $\boldsymbol{D_L(0,\vec{p})}$ **does not depend on $\boldsymbol{\mu}$ so much**.

At high temperature ($T = 103, 124$ MeV): $\boldsymbol{D_L(0,\vec{p})}$ ***decreases*** **as $\boldsymbol{\mu}$ increases**.

Chemical potential dependence of screening masses

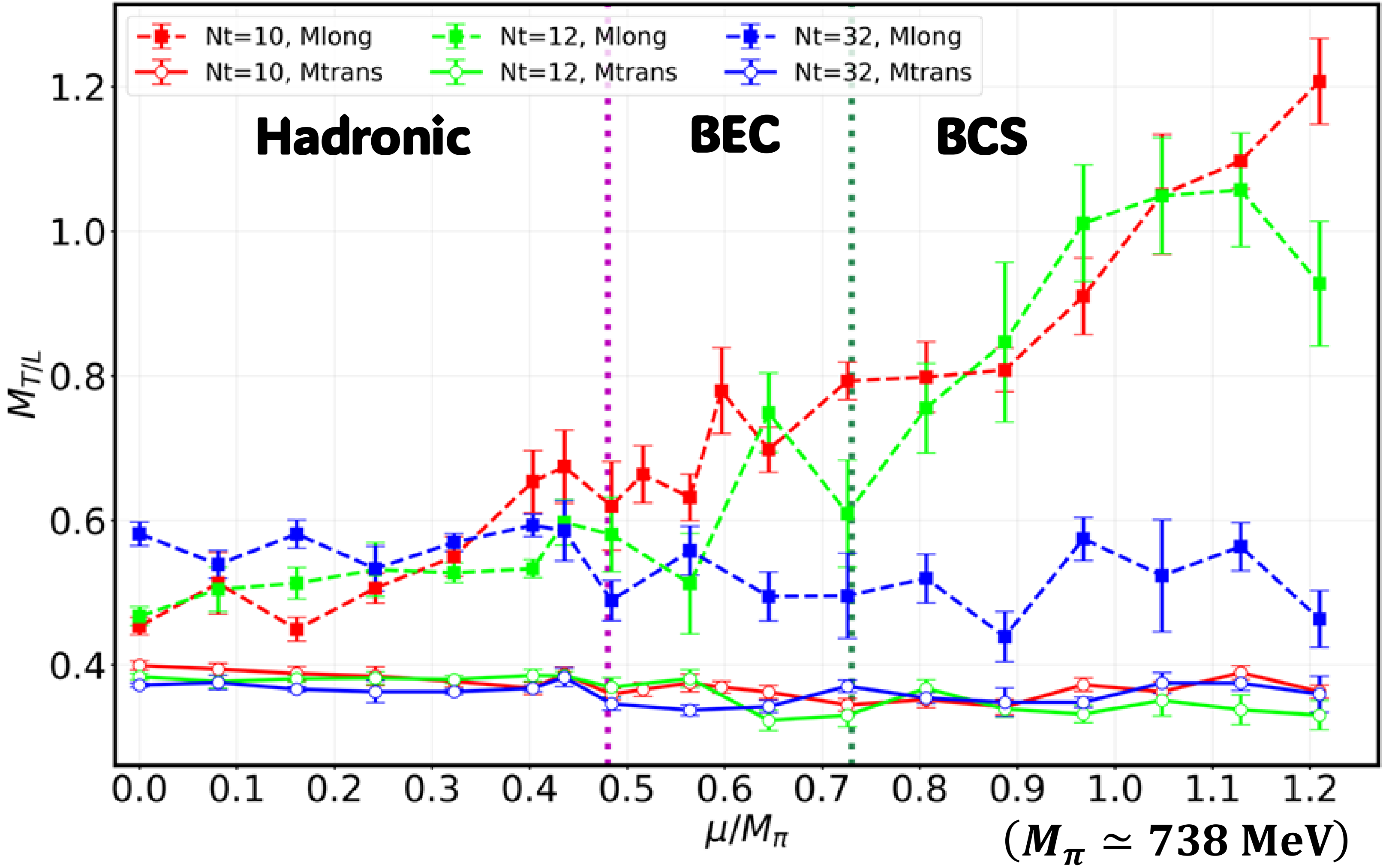

$(M_\pi \simeq 738$ **MeV**$)$

Electric mass:

- **At high T** (103, 124 MeV)
  M_L increase with μ.

- **At low T** (39 MeV)
  M_L is constant for μ.

Magnetic mass:

- Independent of μ for all T.

Chemical potential dependence of screening masses

British group:

$V \simeq 12^3 \times 24, 16^3 \times 32$

$(\beta = 1.9, 2.1$, plaquette, 2-flavor WF)

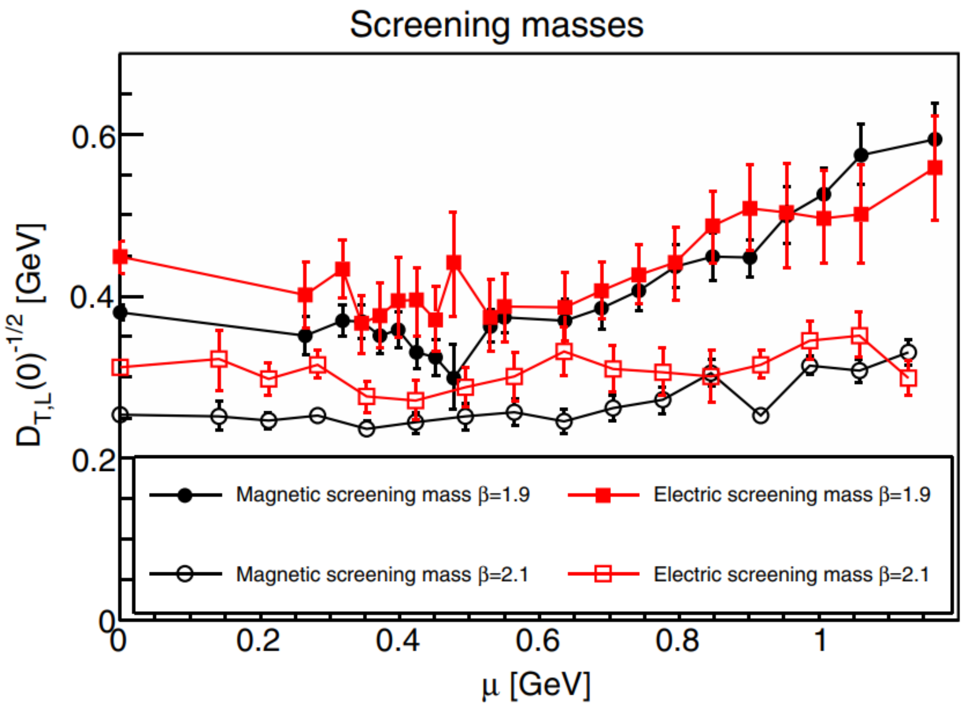

Tamer Boz, Ouraman Hajizadeh, Axel Maas, and Jon-Ivar Skullerud, Phys. Rev. D **99**, 074514(2019)

$T \sim 44$ MeV

Low temperature

Russian group :

$V \simeq 32^3 \times 32$

$(\beta = 1.8$, tree−level improved Symanzik, 2-flavor staggered)

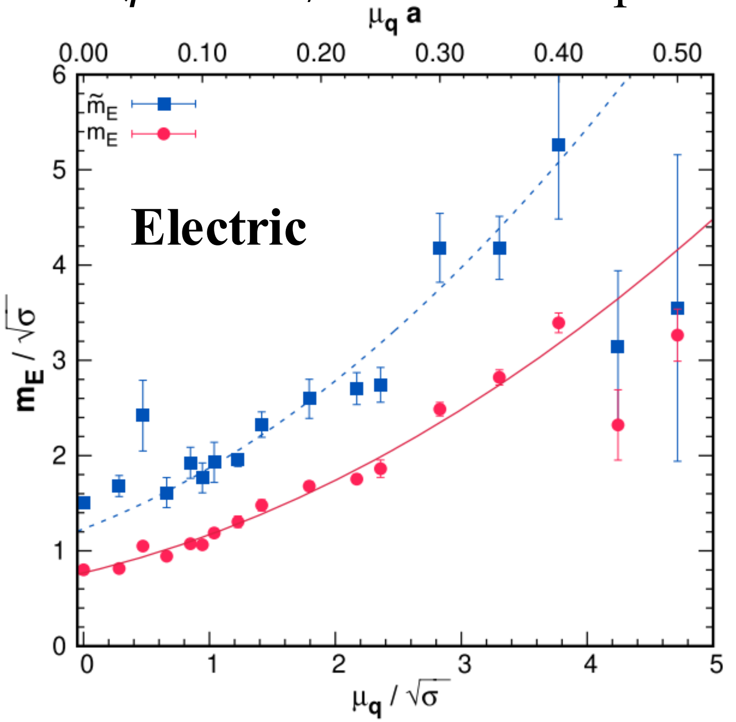

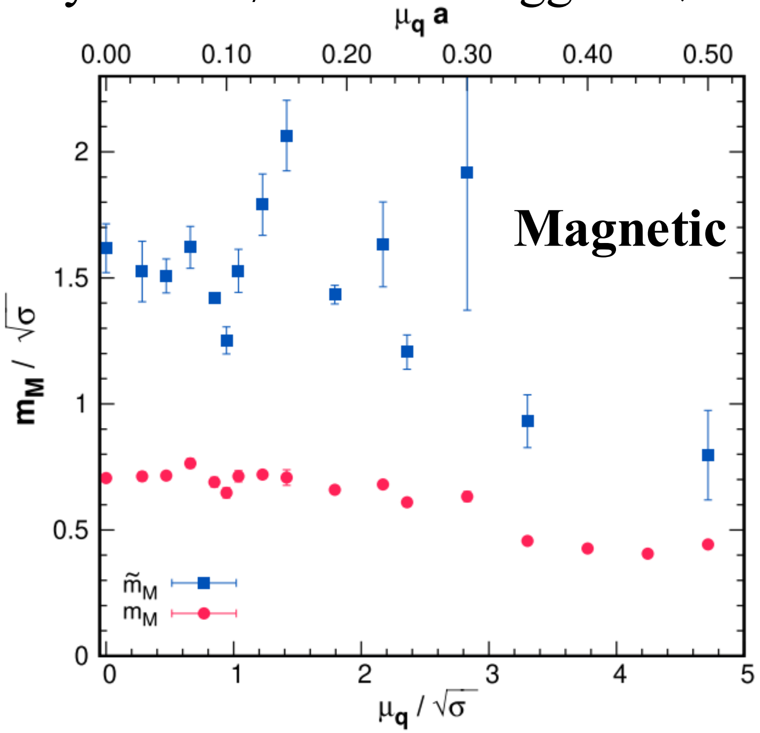

V. G. Bornyakov, V. V. Braguta, A. A. Nikolaev, R. N. Rogalyov, Phys. Rev. D **102**, 114511 (2020)

$T \sim 140$ MeV

High temperature

Chemical potential dependence of screening masses

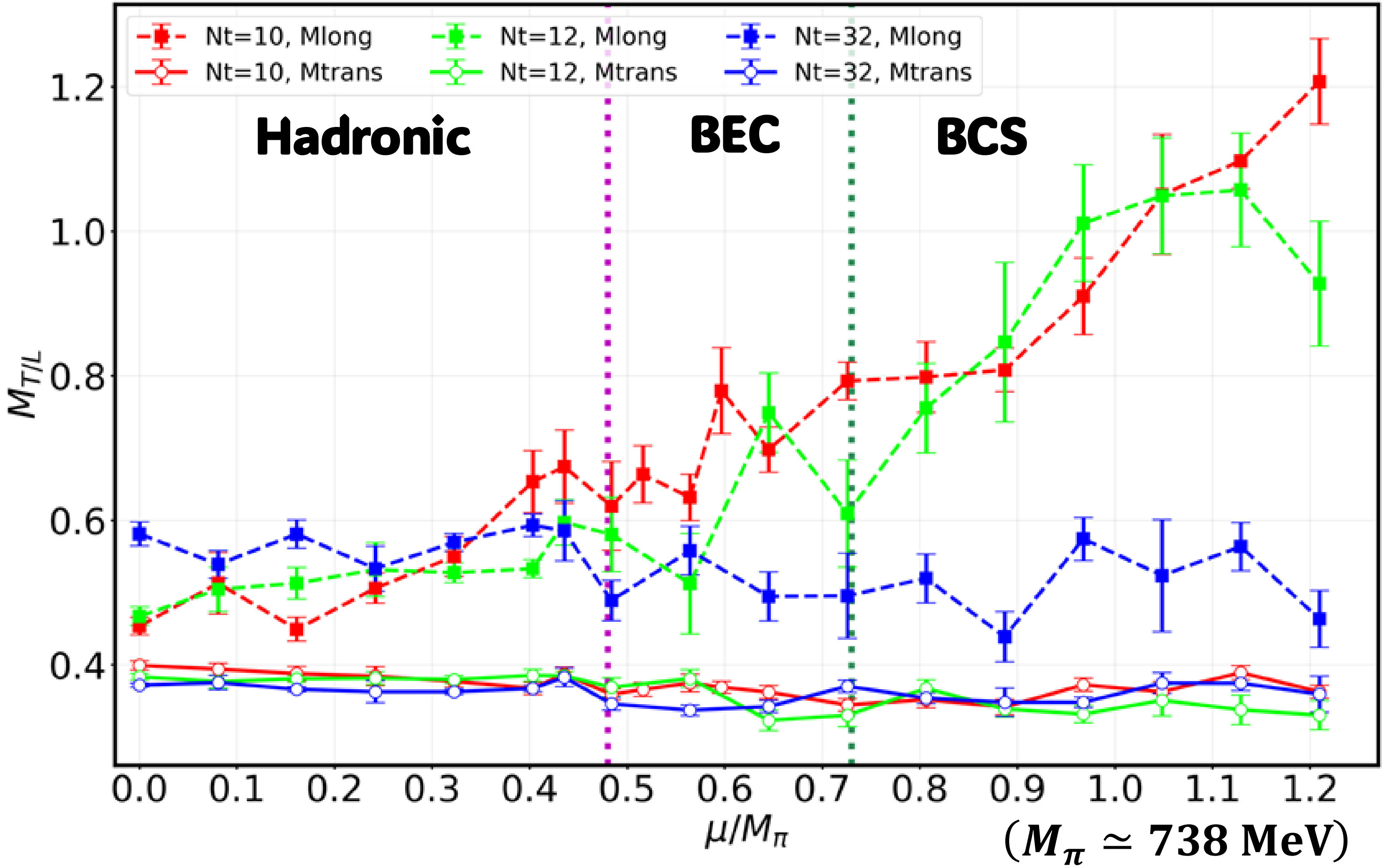

($M_\pi \simeq$ 738 MeV)

Electric mass:

- **At high T** (103, 124 MeV)
  ***M_L* increase with *μ*.**
- **At low T** (39 MeV)
  ***M_L* is constant for *μ*.**

Magnetic mass:

- Independent of μ for all T.

The electric mass exhibits a strong μ dependence if T is high.

Summary

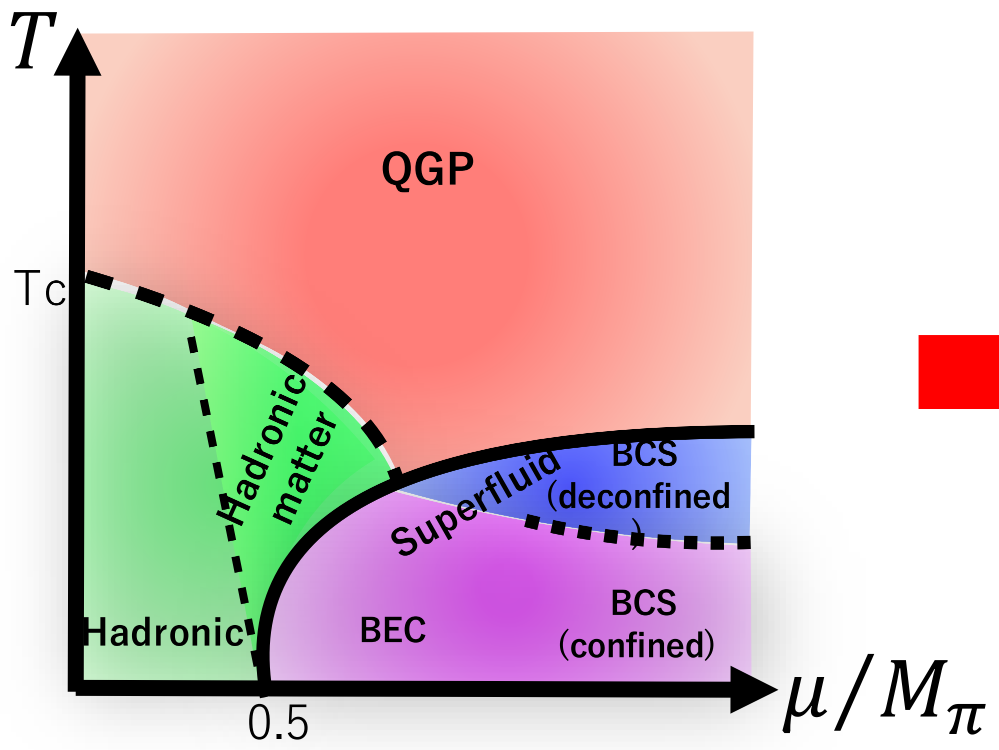

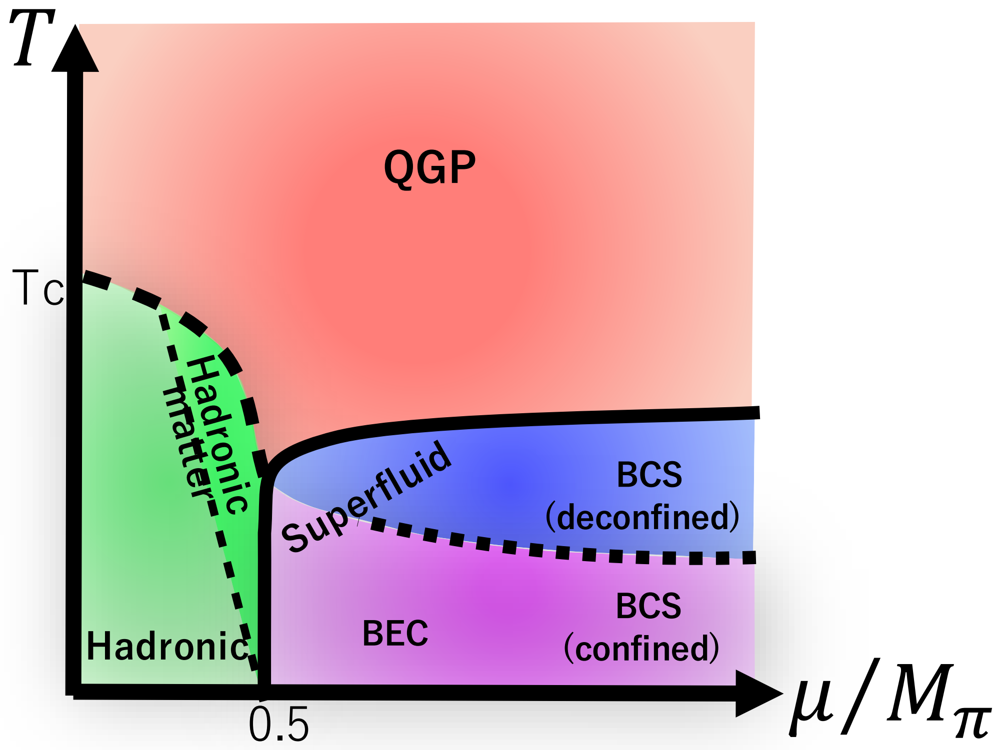

We investigated gluon propagators and screening masses in dense-QC$_2$D, and found that

1. Magnetic dressing function does not depend on chemical potential strongly.
2. The electric dressing function is also independent of μ at low temperature, while it increases as μ increases at high temperature.

The electric mass exhibits a strong μ dependence in deconfinement regions.

Backup

$j \to 0$ extrapolation: magnetic mass

$32^3 \times 32$ (39 MeV)

$32^3 \times 12$ (103 MeV)

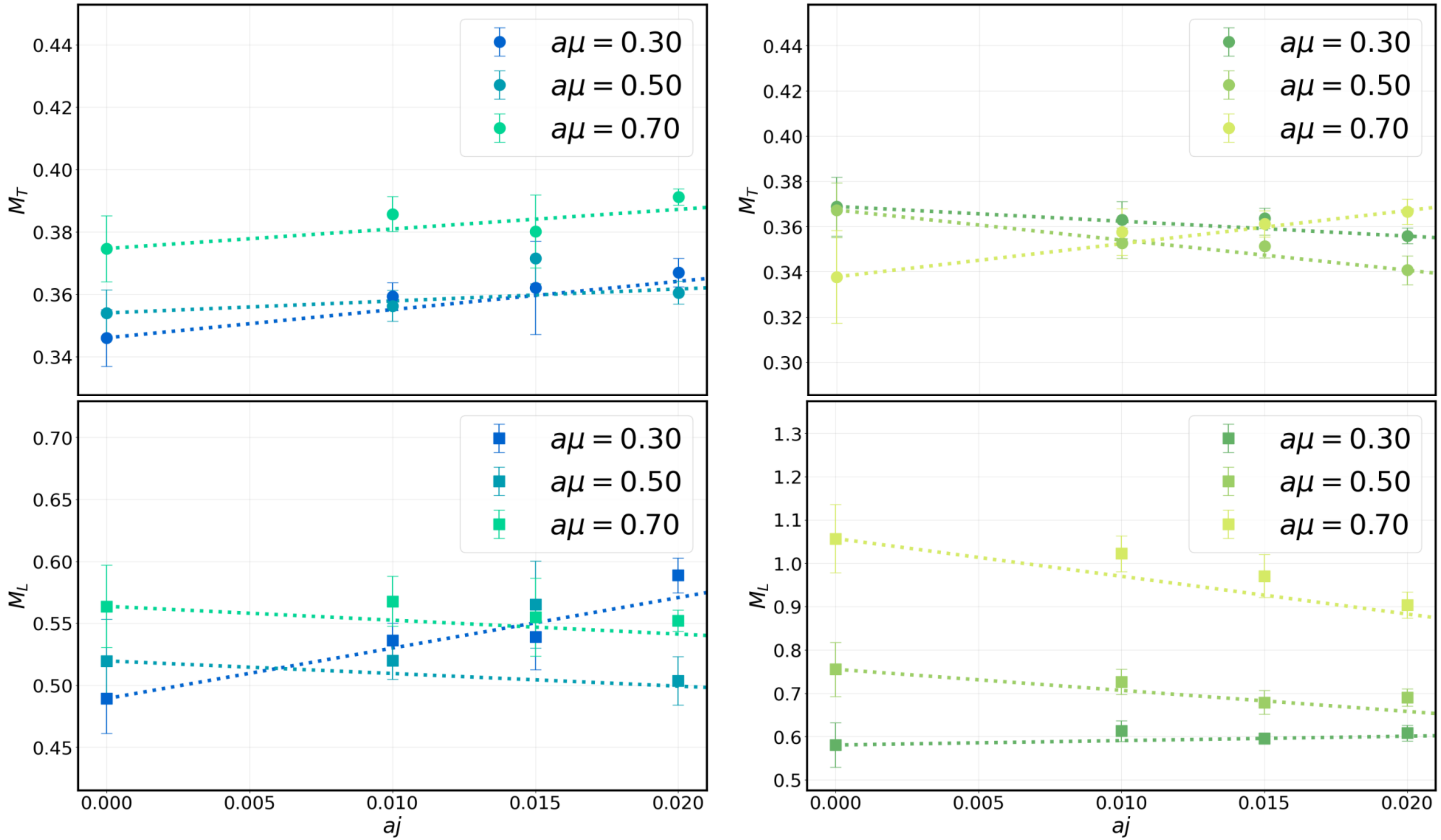

Gluon screening mass:

$$M_{\mathrm{T/L}} \equiv \frac{1}{\sqrt{D_{\mathrm{T/L}}(0, \vec{0})}}$$

1. Prepare 10 binned samples
2. Perform extrapolation for each samples.
3. Calculate extrapolated masses and their error by Jackknife method.

Qualitative comparison with effective theory

Magnetic dressing function $D_T(0,\vec{p})$:

Y. Kurebayashi, T. Kojo and D. Suenaga, Universe 2025, 11(11), 357 (arXiv:2509.20874 [hep-ph])

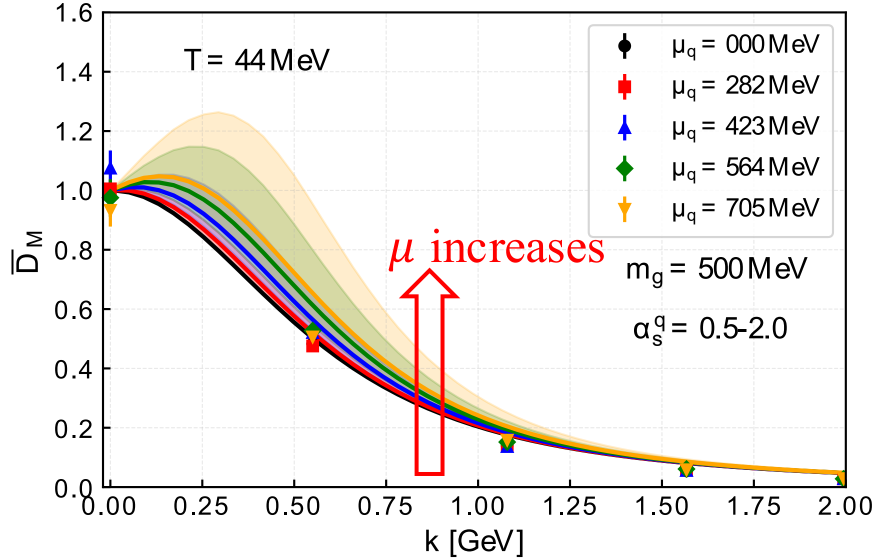

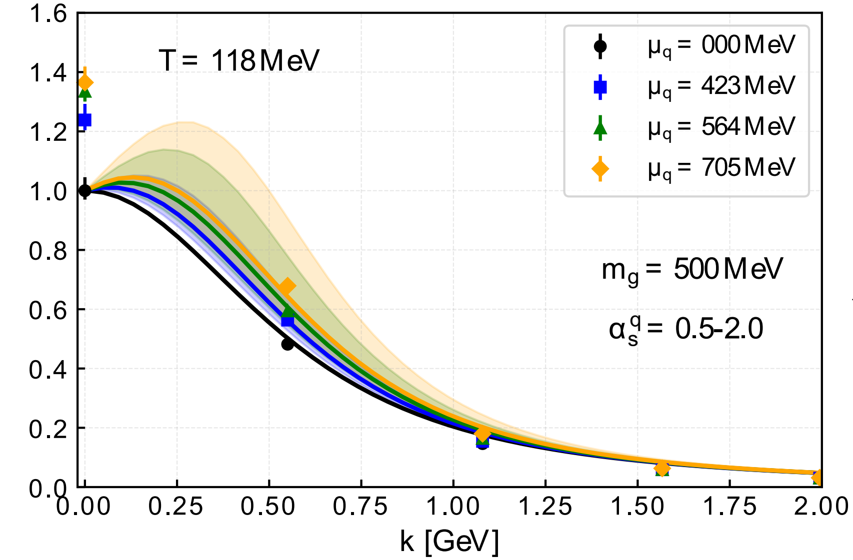

Magnetic:

At any T, D_T increases with μ.

Electric dressing function $D_L(0,\vec{p})$:

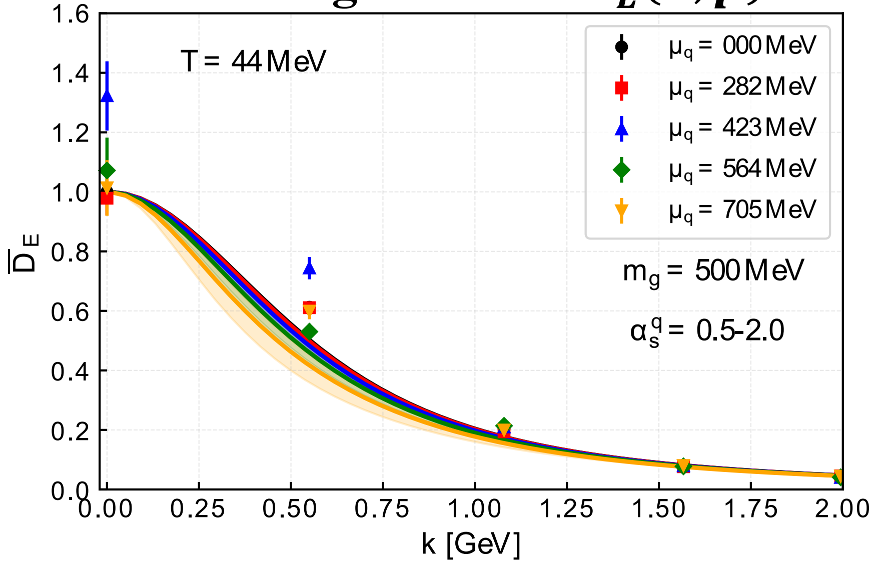

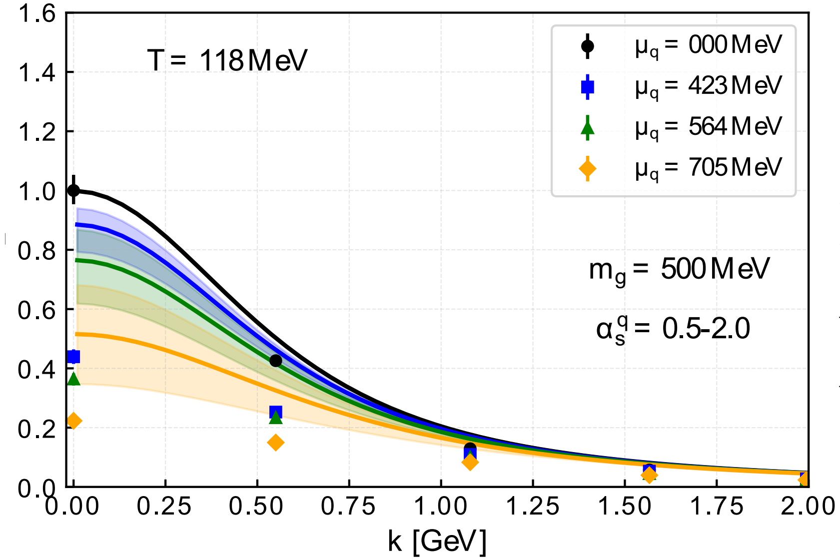

Electric:

At low T, D_L is indep. of μ.

At high T, D_L decreases with μ.

Chemical potential dependence of Polyakov loop

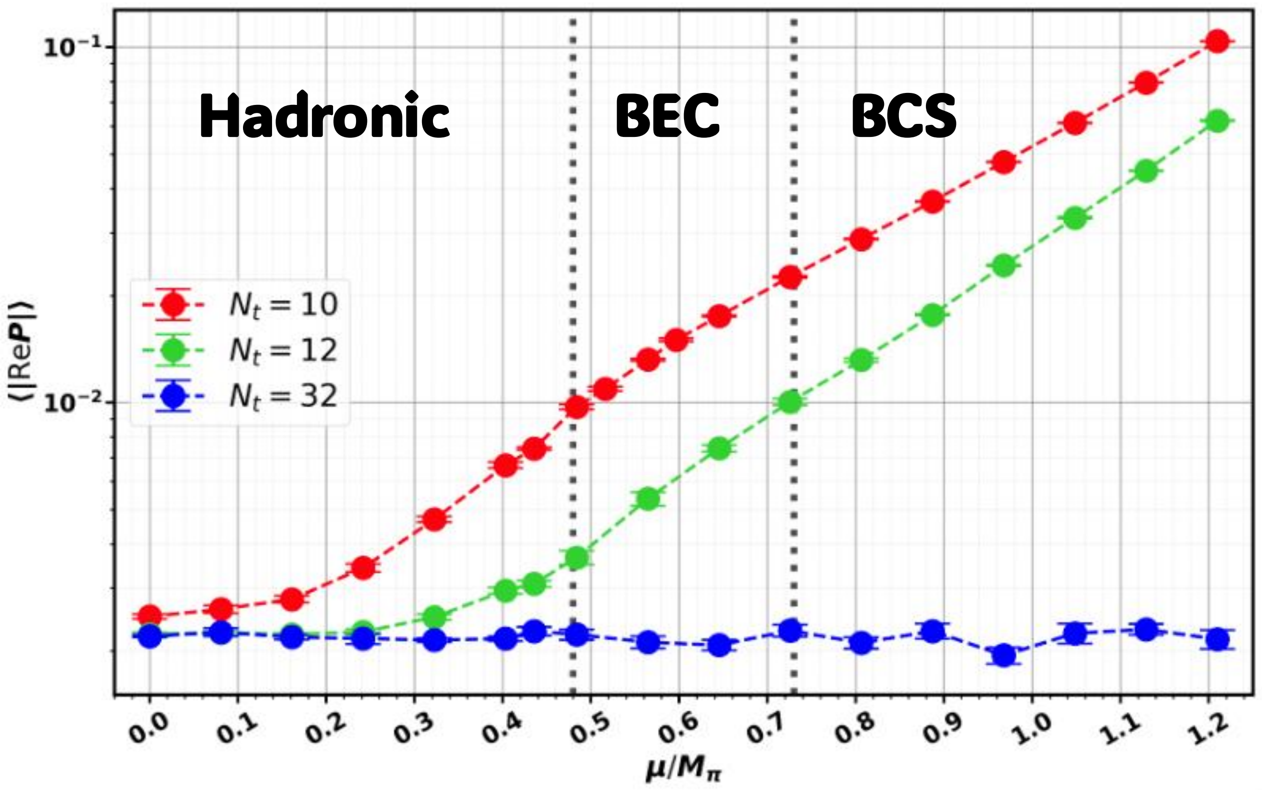

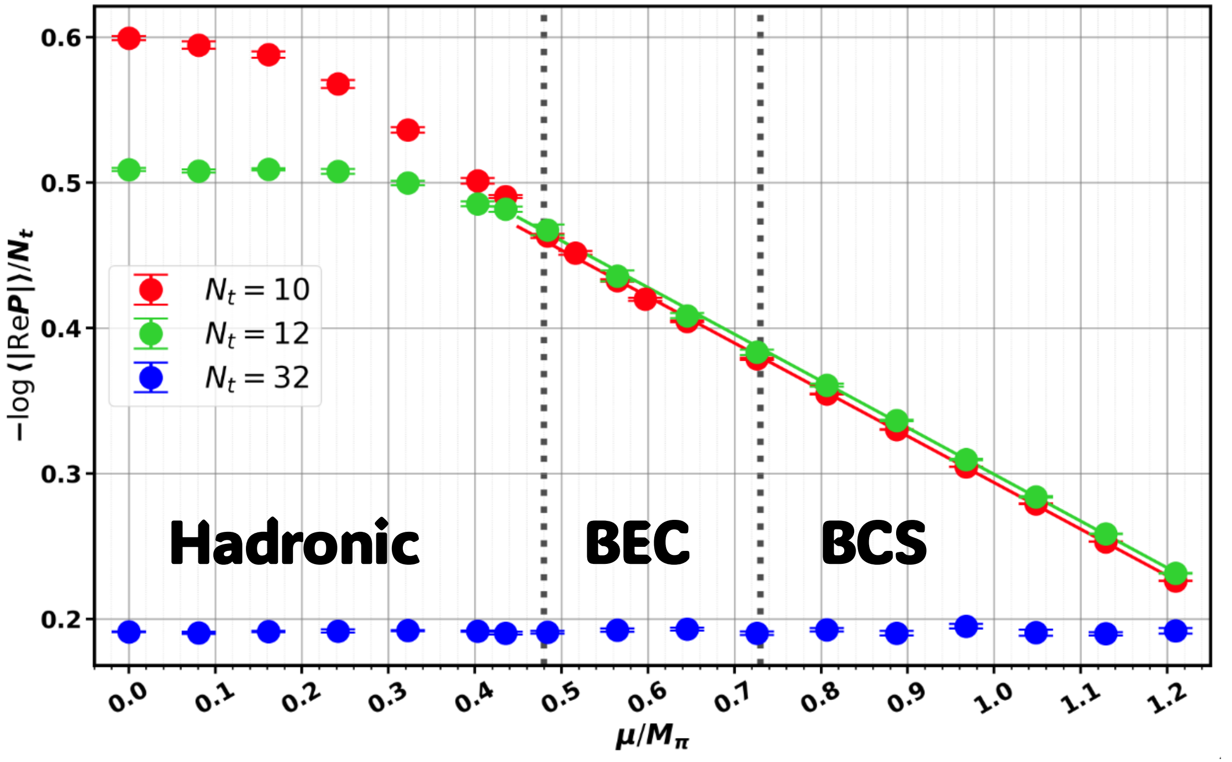

At high T and μ region,

$$\langle|\mathrm{Re}P|\rangle \propto e^{c\mu/T}$$

The slopes at the high-μ region ($\mu/M_\pi > 0.48$) are common in $T > 100$ MeV.

Comparison of phase diagram and Polyakov loop

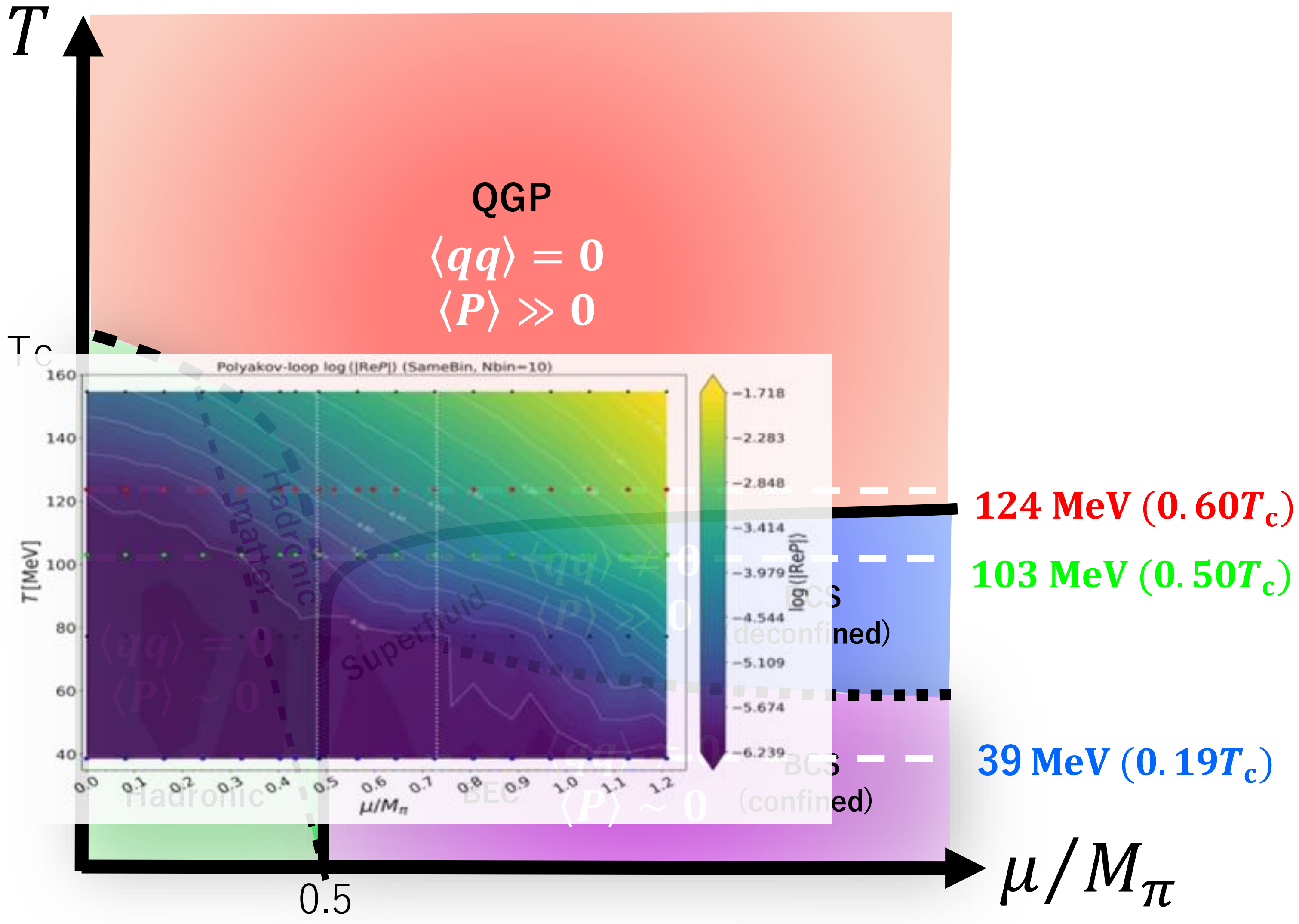

$\boldsymbol{M_\pi \simeq}$ **738 MeV** $(aM_\pi = 0.620)$.